

# Highly Efficient Terahertz Photoconductive Detectors Operating at $\mu\text{W}$ -level Gate Powers

LUCY L HALE,<sup>1,\*</sup> C THOMAS HARRIS,<sup>2,3</sup> TING SHAN LUK,<sup>2,3</sup> SADHVIKAS J ADDAMANE,<sup>2,3</sup> JOHN L RENO,<sup>2,3</sup> IGAL BRENER,<sup>2,3</sup> AND OLEG MITROFANOV,<sup>1,2</sup>

<sup>1</sup>University College London, Electronic and Electrical Engineering, London WC1E 7JE, United Kingdom

<sup>2</sup>Center for Integrated Nanotechnologies, Sandia National Laboratories, Albuquerque, New Mexico 87123, USA

<sup>3</sup>Sandia National Laboratories, Albuquerque, New Mexico 87123, USA

\* [lucy.hale@ucl.ac.uk](mailto:lucy.hale@ucl.ac.uk)

Received XX Month XXXX; revised XX Month, XXXX; accepted XX Month XXXX; posted XX Month XXXX (Doc. ID XXXXX); published XX Month XXXX

**Abstract.** Despite their wide use in terahertz (THz) research and technology, the application spectrum of photoconductive antenna (PCA) THz detectors is severely limited due to the relatively high optical gating power requirement. This originates from poor conversion efficiency of optical gate beam photons to the photocurrent in materials with sub-picosecond carrier lifetimes. Here, we show that an ultra-thin (160 nm), perfectly absorbing low-temperature grown GaAs metasurface can be used as the photoconductive channel to drastically improve the efficiency of THz PCA detectors. This is achieved through perfect absorption of the gate beam in a significantly reduced photoconductive volume, enabled by the metasurface. This study demonstrates that sensitive THz PCA detection is possible using optical gating powers as low as  $5 \mu\text{W}$  – three orders of magnitude lower than gating powers used for conventional PCA detectors. We show that significantly higher optical gate powers are not necessary for optimal operation of such detectors as the sensitivity to THz field improves only marginally. This class of efficient PCA THz detectors opens doors for THz applications with low gate power is requirements. © 2021 Optical Society of America under the terms of the OSA Open Access Publishing Agreement.

Application of terahertz (THz) technology is broadening rapidly fueled by recent advances in THz telecommunication research [1, 2], THz imaging and spectroscopy [3–5], and in new materials and devices for THz generation [6, 7] and detection [8, 9]. Photoconductive antennas (PCAs) are one of the most established and widely used detectors of THz radiation [10, 11]. Their versatile room-temperature operation and broadband coherent detection capability have enabled numerous THz spectroscopy and imaging studies. Wider application of PCAs, for example in THz detector arrays, has been limited however, partly due to inefficient use of

gate photons required for operation of PCA detectors: approximately  $10^6$ - $10^8$  near-IR gate pulse photons are used to generate a single electron of the detector photocurrent.

The majority of past efforts to improve PCA efficiency have used plasmonic structures such as metallic interdigitated contacts, nanorods or nanoantennas, which were integrated onto the photoconductive region [12–19]. However, metallic elements introduce ohmic losses and may deteriorate the electronic properties of the detectors (e.g. by reducing the off-state dark resistance, which affects the detector sensitivity). In another approach, optical cavities have been designed to trap gate photons in a thin photoconductive layer and enhance absorption [20–22] [13–16]. Recently, all-dielectric perfectly absorbing metasurfaces have been proposed to replace the bulk photoconductive layer in THz detectors [8], [23–25]. Such metasurfaces can enhance the efficiency through increasing absorption of gate photons and eliminating reflection. Furthermore, metasurfaces also allow engineering of the electronic properties of PCA detectors, and therefore promise sensitive THz detection at significantly reduced gating powers.

A photoconductive metasurface designed to support two degenerate Mie modes in each meta-atom can enhance conversion of near-IR gating beam photons to photocarriers. Practically complete absorption of the beam can be achieved if, in addition, the critical coupling condition is satisfied [26,27]. This was first realized using in-plane and out-of-plane magnetic dipole (MD) Mie modes in a 200 nm thick metasurface [8]. It enabled operation of THz detectors with  $\sim 100 \mu\text{W}$  of gating power. However, exciting both these modes simultaneously requires breaking of the metasurface symmetry. More recently, a symmetric metasurface design was proposed using degenerate electric dipole (ED) and MD modes [23]. In addition to enabling perfect absorption at a desired wavelength, this new design is thinner (160 nm) and enables electronic conduction within the entire metasurface plane in contrast to previous asymmetric designs.

Here, we show that using this symmetric metasurface design as photoconductive layer in a THz PCA detector enables operation of THz PCA detectors with  $\mu\text{W}$ -level optical gate powers. We

investigate the detector performance in the low gating power regime and find that the dynamic range of  $\sim 10^6$  can be achieved with only  $5 \mu\text{W}$  of gate power - 3 orders of magnitude smaller than the operation power required for bulk THz PCA detectors. Furthermore, we show that significantly higher optical gate powers are not necessary for optimal operation of such detectors as the sensitivity to THz field improves only marginally. These highly efficient PCA THz detectors can open doors to previously impossible THz applications where  $\mu\text{W}$ -level gate power operation is essential, such as THz detector arrays for imaging applications, cryogenic applications and large area THz modulators with ultrafast switching times.

A microscope image of the PCA THz detector with the integrated metasurface can be seen in Fig. 1, along with a close-up SEM of the photoconductive metasurface region. The metasurface consists of interconnected low-temperature grown (LT) GaAs nano-scale channels. The metasurface thickness is only 160 nm, several times thinner than the absorption length. Two metallic THz dipole antennas with a  $3 \mu\text{m}$  gap are fabricated directly on top of the LT-GaAs metasurface. After the antenna deposition, the device is bonded to a sapphire substrate using epoxy. More details of the metasurface and detector fabrication can be found in the Supplemental Document.

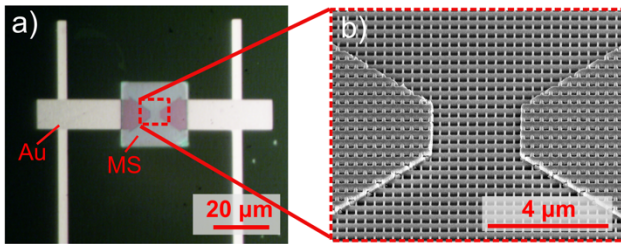


**Fig. 1.** Metasurface PCA Detector: a) Microscope image showing the photoconductive antenna with transmission lines and the metasurface (MS) at the center. b) SEM image of central metasurface region in (a).

The metasurface design is shown in Fig. 2. Each unit cell supports the ED mode with the dipole vector in the y-direction and the MD mode with the dipole vector in the x-direction. Both modes can be excited directly by a linearly polarized (in the y-direction) light (Fig. 2a). The metasurface parameters are chosen so that absorption is maximised at the operation wavelength of the Ti:Sapphire laser (780 nm) (see Suppl. 1). A close-up SEM of this metasurface is shown in Fig. 2b. The optical transmission spectrum shows a minimum (and thereby maximum absorption) at 780 nm (Fig. 2c). Figure 2d illustrates that the single absorption band seen in Fig. 2b is due to two degenerate modes, which separate if the metasurface thickness is varied. We note that perfect absorption can be achieved also at different wavelengths (Fig. 2d) by tuning the metasurface parameters [23].

After integrating the metasurface with the THz antenna, we first investigate electronic properties of the detector. The  $I/V$  behavior is linear with a dark resistance of  $80 \text{ G}\Omega$  – over an order of magnitude higher than for typical bulk PCA devices. This is due to a small cross-section of the conductive channels. The high dark resistance helps to achieve a high detector sensitivity as it will be shown later.

Next, we evaluate the detector response to the THz field using in a standard THz time domain spectroscopy (TDS) system as shown

in Figure 3c. A Ti:Sapphire laser with 80 MHz repetition rate is used to generate 100 fs pulses centered at 780 nm. A zinc telluride crystal is used for broadband THz generation (500 mW pump modulated at 1.75 kHz). The probe beam is focused onto the antenna gap ( $\text{NA}=0.5$ ; spot size  $\sim 3 \mu\text{m}$ ) to gate the detector. To control the gate power, a half-wave plate and polarizer are introduced into the detector beam path.

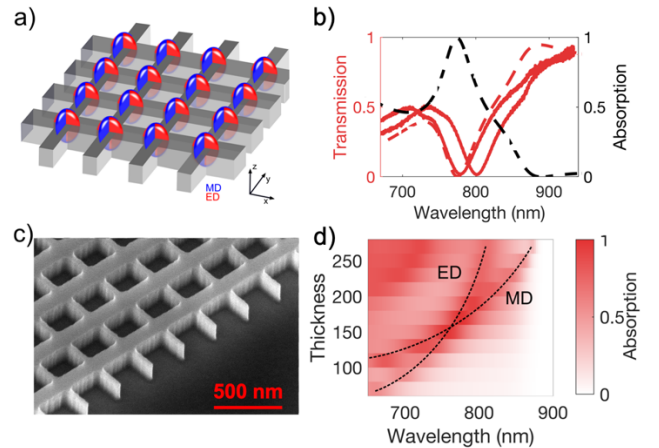


**Fig. 2.** Perfectly Absorbing LT-GaAs Metasurface: a) Schematic of metasurface showing electric (ED, red) and magnetic (MD, blue) dipoles. b) Measured optical transmission of two perfectly absorbing metasurfaces at 780 nm and 800 nm (red solid line) and simulated transmission (red) and absorption (black) of perfectly absorbing metasurface at 780 nm. c) SEM of metasurface at an oblique angle d) Simulated absorption spectra with varying metasurface thickness. Absorption bands due to ED and MD mode absorption are labelled.

Following the excitation of the photoconductive metasurface channel by the gate beam, the resistance switches from a high dark resistance (OFF) state to a low-resistance (ON) state for a fraction of a picosecond, and allows temporally-resolved sampling of incident THz pulses. Figure 3a shows the detected THz waveforms at three  $\mu\text{W}$ -level gate powers:  $5 \mu\text{W}$ ,  $10 \mu\text{W}$  and  $40 \mu\text{W}$ . Even for the lowest tested power of  $5 \mu\text{W}$  – approximately 3 orders of magnitude lower than powers used for bulk PCAs – the THz pulse waveform shows excellent signal-to-noise ratio (SNR). Normalized Fourier spectra of the three waveforms are shown in Fig. 3b showing a dynamic range of  $\sim 10^6$  achieved for all three gating powers. This excellent low gate power operation indicates an improvement in conversion efficiency of gate pulse photons to the THz wave-driven photocurrent.

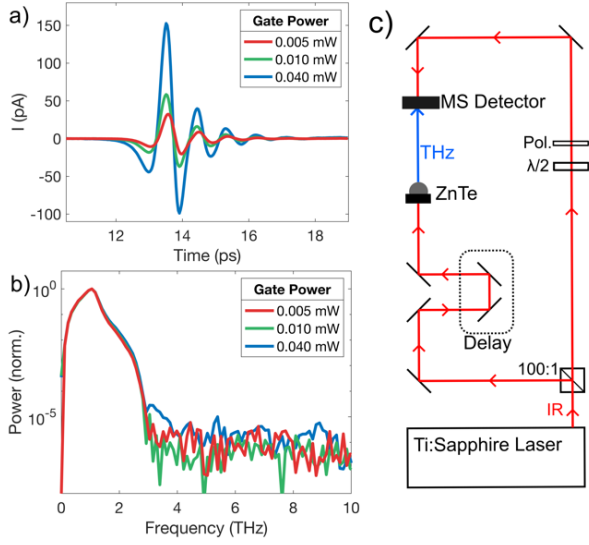


**Fig. 3.** Terahertz Measurements: a) Detected waveforms emitted from a ZnTe crystal, measured at different gating powers b) Power spectral density (PSD) obtained by Fourier transforming the waveforms shown in (a). c) Schematic of THz-TDS measurement set-up.

To evaluate the impact of the improvement in conversion efficiency on the detector performance, we now consider the effect of the optical gate power on the photocurrent response to the THz field and the detector noise. First, we discuss the photocurrent response. It has been shown that bulk PCA devices (both detectors and sources) exhibit a photocurrent saturation behavior, where the photocurrent can be expressed as  $I(P) \propto (P/(P + P_0)) E_{THz}$ , where  $P$  denotes the gating power,  $P_0$  is the saturation power parameter and  $E_{THz}$  is the THz field [10], [28]–[31]. Our metasurface PCA detector follows the same functional behavior: Fig. 4 illustrates the photocurrent at the peak of the THz pulse,  $I_{max}$ , as a function of the gate power. We find a very good agreement with the saturation model  $I_{max} = A(P/(P + P_0))$ , where  $A$  is a constant. However, the saturation power parameter describing this behavior is significantly lower compared to earlier demonstrated THz PCAs (Table. 1). We find that the saturation parameter in our work is only 147  $\mu$ W, whereas conventional bulk THz detectors typically show over one order of magnitude larger saturation powers.

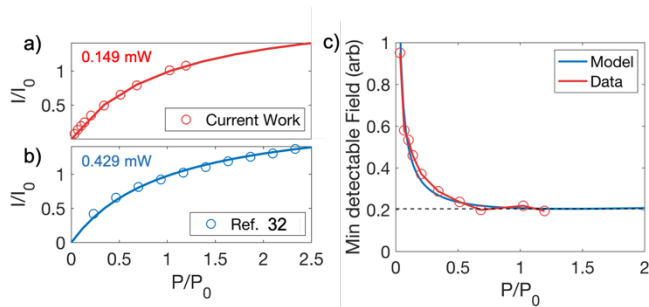


**Fig. 4.** Saturation Characteristics of Metasurface Detectors: a) & b) Peak detected amplitude normalized to the peak amplitude  $I_0$  at saturation power  $P_0$  is plotted against gating power, normalized to the saturation power. Data is fitted to the curve  $A(P/(P + P_0))$  where  $A$  and saturation power  $P_0$  are constants. c) Minimum detectable field as a

function of normalized optical gating power. Calculated using measured RMS noise (red) and model fitted to RMS noise (blue) – see Suppl. 1.

**Table 1. Saturation Power  $P_0$  for LT GaAs PCA THz detectors**

Detector Type	$P_0$ (mW)	Ref.
metasurface/dipole	0.146	This work
metasurface/dipole	0.44(5)	[8]
metasurface/dipole	0.42(9)	[31]
bulk/bow-tie	4.5	[28]
bulk/dipole	2.5	[28]

The sublinear increase of the photocurrent suggests that the optimal performance may be achieved before the onset of saturation. To verify this, we measure the detector noise dependence on the gate power. The detector current is sampled 200 times when  $E_{THz} = 0$  (at a time  $\sim 10$  ps before the arrival of the THz pulse) and the current noise is calculated as the root mean square (RMS) value of the sampled current (see Suppl. for details). The measured noise increases with the optical gate power. For  $P = 0$ , the detector current noise is negligible due to very high dark resistance (i.e. Johnson current noise is negligible) and the measured noise is dominated by the current amplifier input noise. As the gate power is increased the noise increases following approximately a square root dependence on the gate power - characteristic of Johnson noise and shot noise, with both producing comparable contributions (see Supplemental document for details). We quantify the detector detectivity here as the THz field that induces a photocurrent equal to the measured noise current for a given gate power. This lowest detectable THz field is plotted in Fig. 4c as a function of the gate power (see Supplemental document for calculation details). As the optical gate power is increased, the noise equivalent THz field decreases sharply first, however it remains close to a constant value for gate powers above  $\sim P_0/4$ , ( $\sim 30$ - $40 \mu$ W for this detector).

An important conclusion from this analysis is that for gate powers larger than  $\sim 1/4$  of the saturation power  $P_0$ , any improvement in detection sensitivity is marginal. Moreover - at very high gate powers, increasing the gate power is detrimental to the detection sensitivity due to the noise increase with gate power (see Suppl. for detailed calculations). The saturation parameter  $P_0$  therefore can be used as a benchmark for determining the optimal operation gate power for a given PCA detector. The lowest reported saturation behavior with a  $P_0$  value of 0.43,  $\sim 3$  times larger compared to this work (see Fig. 4b), was also achieved with a PC metasurface detector [31].

Our analysis also indicates that the reduced photoconductor volume, which leads to a very high dark resistance, is another factor contributing to high sensitivity at very low gate powers. In this work, the photoconductive volume is only  $\sim 5\%$  of a typical bulk detector whilst still absorbing practically all gate photons. Using results available in the literature, we can generalize that the enhanced absorption and the reduced photoconductive volume in all reported metasurface-type PCA THz detectors play key roles in achieving efficient and sensitive performance [8, 31].

To conclude, sensitive and efficient THz detection is demonstrated for  $\mu$ W-level optical gate powers using PCAs with perfectly-absorbing photoconductive metasurfaces. A THz-TDS dynamic range of  $\sim 10^6$  is achieved at gating powers as low as 5  $\mu$ W.

We show that the photocurrent saturation parameter can be used for evaluation of the optimal operation conditions for THz PCA detectors, where highest sensitivity is achieved with the lowest optical gate power. The saturation power parameter in this work is over an order of magnitude lower compared to bulk PCAs and  $\sim 3$  times lower than in previously demonstrated photoconductive metasurface detectors [31]. The design presented in this paper represents the most efficient PCA THz detector to date to our knowledge. Our results demonstrate that sensitive THz detection is possible at much lower gate powers than commonly used, due to the highly efficient absorption of the gate beam by the metasurface and the reduced photoconductive volume. Such highly efficient detectors could find uses in a wide range of THz spectroscopy and imaging systems – particularly where low gating power is essential, such as in imaging arrays and in cryogenic applications where heating should be minimized.

**Funding.** This work was supported by the U.S. Department of Energy, Office of Basic Energy Sciences, Division of Materials Sciences and Engineering and performed, in part, at the Center for Integrated Nanotechnologies, an Office of Science User Facility operated for the U.S. Department of Energy, Office of Science. Sandia National Laboratories is a multimission laboratory managed and operated by National Technology and Engineering Solutions of Sandia, LLC, a wholly owned subsidiary of Honeywell International, Inc., for the U.S. Department of Energy's National Nuclear Security Administration under Contract No. DE-NA0003525. This paper describes objective technical results and analysis. Any subjective views or opinions that might be expressed in the paper do not necessarily represent the views of the U.S. Department of Energy or the United States Government. OM and LH acknowledge the support of the EPSRC (EP/P021859/1, EP/L015455/1).

**Disclosures.** The authors declare no conflicts of interest.

See Supplement 1 for supporting content.

## References

- [1] T. Nagatsuma, G. Ducournau, and C. C. Renaud, "Advances in terahertz communications accelerated by photonics," *Nat. Photonics*, vol. 10, no. 6, pp. 371–379, 2016.
- [2] H. Elayan, O. Amin, R. M. Shubair, and M. S. Alouini, "Terahertz communication: The opportunities of wireless technology beyond 5G," *Proc. - 2018 Int. Conf. Adv. Commun. Technol. Networking, CommNet 2018*, pp. 1–5, 2018.
- [3] T. L. Cocker *et al.*, "An ultrafast terahertz scanning tunnelling microscope," *Nat. Photonics*, vol. 7, no. 8, pp. 620–625, 2013.
- [4] I. C. Benea-Chelms, F. F. Settembrini, G. Scalari, and J. Faist, "Electric field correlation measurements on the electromagnetic vacuum state," *Nature*, vol. 568, no. 7751, pp. 202–206, 2019.
- [5] M. A. Huber *et al.*, "Femtosecond photo-switching of interface polaritons in black phosphorus heterostructures," *Nat. Nanotechnol.*, vol. 12, no. 3, pp. 207–211, 2017.
- [6] E. T. Papaioannou and R. Beigang, "THz spintronic emitters: A review on achievements and future challenges," *Nanophotonics*, 2021.
- [7] L. Luo *et al.*, "Broadband terahertz generation from metamaterials," *Nat. Commun.*, vol. 5, pp. 1–6, 2014.
- [8] T. Siday *et al.*, "Terahertz Detection with Perfectly-Absorbing Photoconductive Metasurface," *Nano Lett.*, vol. 19, no. 5, pp. 2888–2896, 2019.
- [9] Y. Salamin *et al.*, "Compact and ultra-efficient broadband plasmonic terahertz field detector," *Nat. Commun.*, vol. 10, no. 1, pp. 1–8, 2019.
- [10] M. Tani, K. Sakai, and H. Mimura, "Ultrafast photoconductive detectors based on semi-insulating GaAs and InP," *Japanese J. Appl. Physics, Part 2 Lett.*, vol. 36, no. 9 A/B, 1997.
- [11] P. U. Jepsen, R. H. Jacobsen, and S. R. Keiding, "Generation and detection of terahertz pulses from biased semiconductor antennas," *J. Opt. Soc. Am. B*, vol. 13, no. 11, p. 2424, 1996.
- [12] S.-G. Park, Y. Choi, Y.-J. Oh, and K.-H. Jeong, "Terahertz photoconductive antenna with metal nanoislands," *Opt. Express*, 2012.
- [13] X. Li, N. T. Yardimci, and M. Jarrahi, "A polarization-insensitive plasmonic photoconductive terahertz emitter," *AIP Adv.*, vol. 7, no. 11, 2017.
- [14] B. Heshmat *et al.*, "Nanoplasmonic terahertz photoconductive switch on GaAs," *Nano Lett.*, vol. 12, 2012.
- [15] F. Fesharaki *et al.*, "Plasmonic Antireflection Coating for Photoconductive Terahertz Generation," *ACS Photonics*, vol. 4, no. 6, pp. 1350–1354, 2017.
- [16] A. Jooshesh *et al.*, "Nanoplasmonics enhanced terahertz sources," *Phys. Rev. Lett.*, vol. 53, no. 216, pp. 2424–2436, 2014.
- [17] S. G. Park, K. H. Jin, M. Yi, J. C. Ye, J. Ahn, and K. H. Jeong, "Enhancement of terahertz pulse emission by optical nanoantenna," *ACS Nano*, 2012.
- [18] C. W. Berry, N. Wang, M. R. Hashemi, M. Unlu, and M. Jarrahi, "Significant performance enhancement in photoconductive terahertz optoelectronics by incorporating plasmonic contact electrodes," *Nat. Commun.*, 2013.
- [19] N. M. Burford and M. O. El-Shenawee, "Review of terahertz photoconductive antenna technology," *Opt. Eng.*, 2017.
- [20] G. Georgiou, C. Geffroy, C. Bäuerle, and J. F. Roux, "Efficient Three-Dimensional Photonic-Plasmonic Photoconductive Switches for Picosecond THz Pulses," *ACS Photonics*, vol. 7, pp. 1444–1451, 2020.
- [21] M. Billet, P. Latzel, F. Pavanello, G. Ducournau, J.-F. Lampin, and E. Peytavit, "Resonant cavities for efficient LT-GaAs photoconductors operating at  $\lambda_{\text{L}} = 1550 \text{ nm}$ ," *Cit. APL Photonics*, vol. 1, 2016.
- [22] N. T. Yardimci, S. Cakmakcayan, S. Hemmati, and M. Jarrahi, "High-Power photoconductive terahertz source enabled by three-dimensional light confinement," *Int. Conf. Infrared, Millimeter, Terahertz Waves, IRMMW-THz*, pp. 4–5, 2017.
- [23] O. Mitrofanov *et al.*, "Perfectly absorbing dielectric metasurfaces for photodetection," *APL Photonics*, vol. 5, no. 10, 2020.
- [24] L. L. Hale *et al.*, "Perfect absorption in GaAs metasurfaces near the bandgap edge," *Opt. Express*, vol. 28, no. 23, p. 35284, 2020.
- [25] J. R. Piper, V. Liu, and S. Fan, "Total absorption by degenerate critical coupling," *Appl. Phys. Lett.*, vol. 104, no. 25, 2014.
- [26] R. Alaea, M. Albooyeh, and C. Rockstuhl, "Theory of metasurface based perfect absorbers," *J. Phys. D: Appl. Phys.*, vol. 50, no. 50, pp. 1–14, 2017.
- [27] R. Yano, H. Gotoh, Y. Hirayama, S. Miyashita, Y. Kadoya, and T. Hattori, "Terahertz wave detection performance of photoconductive antennas: Role of antenna structure and gate pulse intensity," *J. Appl. Phys.*, vol. 97, no. 10, 2005.
- [28] J. T. Darrow, X. C. Zhang, D. H. Auston, and J. D. Morse, "Saturation Properties of Large-Aperture Photoconducting Antennas," *IEEE J. Quantum Electron.*, vol. 28, no. 6, pp. 1607–1616, 1992.
- [29] S. Rihani *et al.*, "Effect of defect saturation on terahertz emission and detection properties of low temperature GaAs photoconductive switches," *Appl. Phys. Lett.*, vol. 95, no. 5, 2009.
- [30] M. Tani, S. Kono, M. Nakajima, M. Iida, and K. Sakai, "Generation and detection of ultrabroadband Terahertz radiation with photoconductive antennas," *Conf. Dig. - 27th Int. Conf. Infrared Millim. Waves, IRMMW 2002*, pp. 125–126, 2002.
- [31] O. Mitrofanov, T. Siday, R. J. Thompson, T. S. Luk, I. Brener, and J. L. Reno, "Efficient photoconductive terahertz detector with all-dielectric optical metasurface," *APL Photonics*, vol. 3, no. 5, p. 051703, 2018.

